Experiment study on dryout characteristics and thermal resistance analysis of two-phase closed thermosiphon(TPCT)

Junjie Wang[1], Shuo Lin[2], Hanzhong Tao[3], Yannan Li [4,*]

School of energy science and Engineering, Nanjing Tech University, Jiangsu 211816, China

*Corresponding author: liyannan@njtech.edu.cn (Yannan Li)

Abstract:

This study aims to explore the dryout characteristics of two-phase closed thermosiphon (TPCT). It involves the design and experimentation on low-liquid filled heat pipes. We investigated the effects of different fill ratios (FR), heating water temperatures, and cooling water flow rates on the start-up characteristics of TPCT. Based on the network model, we proposed an analytical expression for the thermal resistance (R) of TPCT and provided an explanation of the various thermal resistance components. This research expands our understanding of dryout and provides insights for optimizing heat pipe design and addressing heat conduction issues with low FR.

Keywords: *Dryout, Evaporate, Condensation, Thermal resistance, Empirical formula.*

1. Introduction

A heat pipe is a device that achieves heat transfer by evaporating and condensing a working material in a sealed container. Due to its low thermal resistance (R), excellent isothermal performance, diverse structures, and other advantages, it is widely used in electronic cooling and waste heat recovery applications. Heat pipes are primarily composed of an evaporator and a condenser. In the evaporating section, heat is transferred from the external environment to the internal working medium through the wall. The working material evaporates and carries the heat to the condensing section, which releases it to the external environment through the wall. The vapor then condenses back into a liquid and flows back to the evaporating section, enabling rapid heat transfer through circulation. There are several factors that can affect the performance of heat pipes, including thermal load, working material type, fill ratio (FR), length and diameter of the heat pipes, and the length of the evaporating and condensing sections [1] [2]. In light of these factors, extensive research has been conducted by scholars both domestically and internationally on heat pipes.

Several researchers have investigated the effects of various parameters related to heat pipes, such as fill ratio (FR), the type of working medium, and the presence of a liquid core, on the thermal R of heat pipes. Alizadeh [3] conducted experiments to measure the temperature distribution and temperature difference. The findings revealed that increasing the FR value leads to a decrease in R. Alammar [4] discovered that a heat pipe with 100% FR has approximately 200% higher R compared to a heat pipe with 25% FR. Chen [5] compared the thermal performance of heat pipes and capillary tubes (THPCT) and TPCT by considering R and the heat transfer coefficient. The results showed that the addition of glass beads improved the evaporative heat transfer coefficient and reduced the overall R. Mozumder [6] and colleagues evaluated the performance of heat pipes using water, methanol, and acetone as working fluids. They studied the effect of FR and determined the optimal FR based on lower temperature difference and R, as well as a higher heat transfer coefficient. Guichet [7] investigated the thermal performance of TPCT using water, ethanol, and ethylene glycol as working fluids.

Researchers have conducted a series of studies on various working conditions, including heat load, coolant flow rate, and angle of inclination, to examine their impact on the R of heat pipes. Alizadeh [3] discovered that increasing the coolant flow rate leads to an increase in R. Alammar [4] found that the R of TPCT is minimized at a heat load of 50W. Zhang [8] investigated the influence of the angle of inclination and observed that the internal start-up temperature difference in TPCT varies with this angle. The influence of the R of the cross-section of the heat pipe wall was found to be relatively small. Furthermore, the R of the evaporator, adiabatic section, and condenser surfaces also varies with the inclination angle. The total R of TPCT is minimized at an inclination angle of 20°. Mozumder [9] and colleagues conducted research on the R and heat transfer coefficient of heat pipes by varying the heat input. Guichet [10] considered factors such as inclination angle, heat input, and cooling water flow rate. They investigated the thermal efficiency of TPCT and found that the inclination angle and heat input have a significant impact on TPCT's thermal efficiency.

In the design of heat pipes, optimizing the thermal performance and improving heat transfer efficiency can be achieved by considering factors such as heat power, fill ratio (FR), inclination angle, heat input, and wick structure. However, there is an aspect that has not received sufficient attention, which is the dryout performance of the heat pipe. Current research predominantly focuses on the performance of heat pipes under normal operating conditions, while the occurrence of dryout in the evaporation section has been relatively understudied. This knowledge gap may lead to an incomplete understanding of the behavior of R and heat transfer characteristics of heat pipes.

Therefore, to gain comprehensive insights into the performance of heat pipes under dryout conditions, it is important to manufacture heat pipes designed for low fill ratios. This will facilitate further studies involving detailed experiments on the behavior of R, heat transfer mechanisms, and heat transfer characteristics of heat pipes under dryout conditions. Additionally, it is crucial to develop more accurate methods for calculating R, considering the influencing factors relevant to dryout conditions, in order to more precisely evaluate and enhance the performance of heat pipes.

2. Modeling methodology

The thermal resistance (R) plays a crucial role in evaluating the heat transfer efficiency of heat pipes. Conducting in-depth research on the behavior of R in heat pipes allows us to understand the factors influencing the heat transfer performance of heat pipes and discover effective methods to reduce R and improve heat transfer efficiency.

Traditional methods for calculating R primarily rely on empirical formulas and simplified heat flow path models. While these methods offer a certain degree of accuracy, their applicability under dryout conditions requires further evaluation. These approximate calculation methods may not fully account for the influence of dryout on the internal heat transfer behavior of heat pipes, thus limiting the accurate assessment of heat pipe performance in dryout conditions.

Figure1 illustrates the working principle of the heat pipe and the R network model. Heat is transferred to the evaporation cross section through the wall surface, causing the working medium to evaporate. The heat is then moved to the condensation cross section through the vapor flow, where it condenses and eventually returns to the evaporation cross section under

the influence of gravity.

Considering the intricate variations of the working medium in the TPCT, we divide it into multiple sections and perform a heat resistance analysis on each section. Based on the network model depicted in Figure1, the total R of the TPCP can be calculated using the following formula [10]:

$$R = R_{\text{ext},e} + R_{\text{ext,c}} + \left[\frac{1}{R_{\text{wall, in}}} + \frac{1}{R_{\text{wall},e} + R_{\text{boiling,e}} + R_{\text{vap,in}} + R_{\text{condensation},c} + R_{\text{wall},c}} \right]^{-1}$$

The calculation formulas of each R are shown in Table1, where subscripts e, a and c refer to the evaporation, adiabatic and condensing sections respectively.

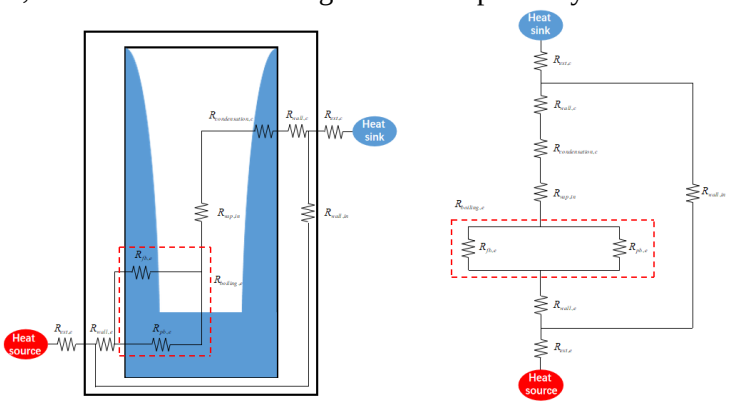

Figure1. Thermal resistance network model. [10]

Table1. Thermal resistances of TPCT

Thermal resistance	Formula
$R_{\text{ext},e}$	$1/\left(h_{0,e}A_{0,e}\right)$
$R_{\text{ext},c}$	$1/\left(h_{0,c}A_{0,c}\right)$
$R_{\text{wall,in}}$	$\left(0.5L_e + L_a + 0.5L_c\right)/\left(A_x k_w\right)$
$R_{\text{wall,e}}$	$\ln\left(D_0/D\right)/\left(2\pi L_e k_w\right)$
$R_{\text{wall},c}$	$\ln\left(D_0/D\right)/\left(2\pi L_c k_w\right)$
$R_{\text{vap},in}$	$T_v\left(P_{v,e} - P_{v,c}\right)/\rho_v i_{lv} q$
$R_{\text{condensation},c}$	$1/\left(h_{\text{condensation}} A_{c,\text{ in}}\right)$
$R_{\text{boiling,e}}$	$\dfrac{1}{h_{pb,e}A_{pb,e} + h_{fb,e}A_{fb,e}}$

From the above equation, it can be seen that the factors influencing the R of a TPCT include the external thermal resistances of the evaporator and condenser sections, the axial and radial wall thermal resistances, boiling resistance, internal vapor resistance, and condensation resistance. Among these, the boiling resistance and condensation resistance need to be numerically predicted.

It can be observed that in predicting the R, not only the condensation heat transfer coefficient needs to be considered but also the heat transfer coefficients of pool boiling and falling film evaporation/falling film boiling. To obtain these parameters, a more detailed understand-

ing of the phenomena occurring within the heat pipe is required.

2.1. Filmwise condensation

As shown in Figure2, vapor undergoes condensation in the condenser section of the TPCT, forming a thin film that starts to descend under the influence of gravity. As the film flows downward, the flow pattern undergoes a transition and becomes more turbulent. There is interaction between the countercurrent vapor flow and the descending film, leading to increased turbulence and even liquid entrainment.

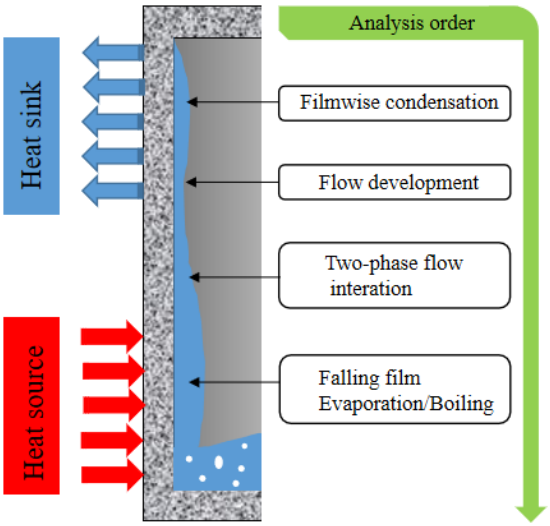

Figure2. Falling film mechanism in a thermosiphon.

To calculate the condensation heat transfer coefficient, it is necessary to determine the condensation film Reynolds number.The number is obtained by Nusselt's theory [11]:

$$R_{f,L_c}=\frac{4\Gamma_{L_c}}{\mu_l}=\frac{4}{\mu_l}\frac{k_l\left(T_{\text{sat}}-T_w\right)}{i_{lv}\delta}L_c=h_{\text{Nusselt}}\frac{4\left(T_{\text{sat}}-T_w\right)L_c}{\mu_l i_{lv}}$$

According to Nusselt's theory [11], the condensation heat transfer coefficient can be estimated. McAdams [12] made corrections to the formula proposed by Nusselt, with a correction factor of 1.13. Kutateladze [13] considered the effect of flow on the coefficient. Butterworth [14] considered waves and used a friction factor in his formula. The empirical formulas presented above are shown in Table2.

Table2. Filmwise condensation heat transfer coefficient

Author	Year	Correlation
McAdams [12]	1942	$h_{\text{Nusselt}}=1.13\left\{\frac{\rho_l\left(\rho_l-\rho_v\right)\mathrm{i_{lv}gk_1}^3}{\mu_l L_c\left(T_{\text{sat}}-T_w\right)}\right\}^{1/4}$
Kutateladze [13]	1963	$h=0.69\,\mathrm{Re}_{f,L_c}^{\ 0.11}\times h_{\text{Nusselt}}$
Butterworth [14]	1981	$h=1.013Re_{f,L_c}^{\ -0.22}k_l\left(\frac{\mu_l^{\ 2}}{\rho_l\left(\rho_l-\rho_v\right)g}\right)^{-1/3}$

2.2. Falling film evaporation

As shown in Figure2, the descending liquid film comes into contact with the heat source, resulting in an increase in temperature. Part of the falling liquid film turns into steam in the middle of the fall, releasing latent heat.

To calculate the falling film evaporation heat transfer coefficient, we first need to determine the Reynolds number of the falling film flow.The number Re_f is derived by Rohsenow [15,16] :

$$Re_f=\frac{4\Gamma}{\mu_t}$$

h can be expressed in terms of h^* by the formula:

$$h^* = \frac{hl_0}{k_i}$$

l_0 can be calculated by the following formula:

$$l_0 = \left(\frac{\mu_l^2}{\rho_l^2 g} \right)^{1/3}$$

To obtain the falling film evaporation heat transfer coefficient, Nusselt [17] derived a formula for calculating $h*$. Subsequently, Wilke [18] developed a formula that relates the Nusselt number to the Reynolds number and the Prandtl number.The empirical formulas presented above are shown in Table3.

Table3. Evaporating film heat transfer coefficient

Author	Year	Correlation
Nusselt [17]	1916	$h* = \frac{k_l}{\delta} = \left(\frac{4\rho_l^2 g k_l^3}{3\mu_l^2} \right)^{1/3} Re_f^{-1/3}$
Wilke [18]	1962	$h^* = 1.76 Re_f^{-1/3}$

As shown in Figure2, falling film boiling occurs in TPCT at higher heat fluxes. By comparing the empirical formulas for falling film evaporation summarized by Chun and Seban [19] and the empirical formula for falling film boiling derived by Fujita and Ueda [20], it is observed that at lower heat fluxes, the formation of film-wise bubbles is limited, and the heat transfer during falling film boiling approaches that during falling film evaporation. The influence of descending film boiling can be neglected when the heat flux is between 0.05 to 0.1W/m^2. Therefore, the effect of falling film boiling on the results is not considered in this study.

3. Experimental setup

In order to accurately assess and understand the phenomena occurring in the TPCT, further experimental investigations are necessary. We designed and constructed a suitable experimental setup that provides a heat source and a cold source, enabling controlled experiments on TPCTs with different FR. This allows for the analysis of the TPCT's start-up characteristics and heat transfer behavior.

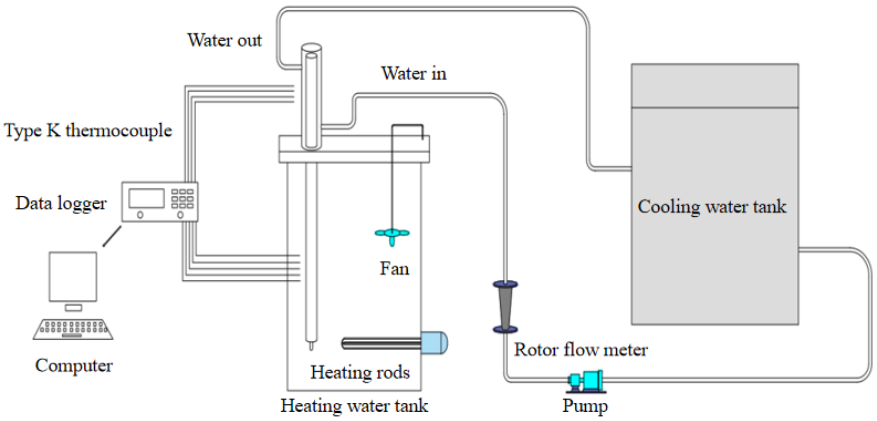

Figure3. Schematic diagram of the experimental setup

As shown in Figure3, the evaporation section of the TPCT is heated by heating the water bath of the tank, which makes the heat more uniform. The tank contains heating rods that regulate the temperature of the heated water. At the same time, a stirring motor was installed in the tank to avoid thermal stratification. The hot water temperature is adjustable. We cover the tank with a foam board and take insulation measures to reduce errors in the experiment.

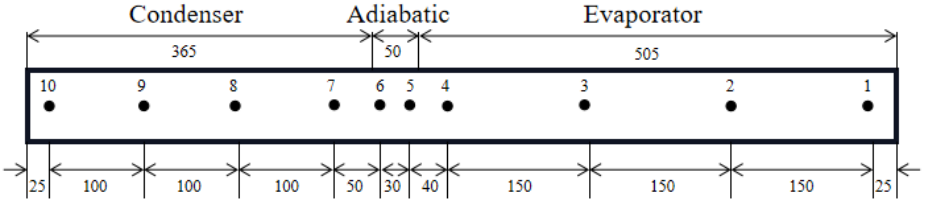

Figure4. Thermocouple layout

The data acquisition system consists of a computer, a 34970A data acquisition instrument, a glass rotor flow meter and twelve pairs of K-type thermocouples. Ten pairs of K-type thermocouples are arranged along the walls of the TPCT along the axis, and two pairs of K-type thermocouples are arranged at the inlet and outle to measure the water temperature.

In the experiment, the TPCT is made of stainless steel. The TPCT has an inner diameter of 16 mm and a wall thickness of 1.5mm. The arrangement of the thermocouples is shown in Figure4. The wall temperature of TPCTs evaporation section (T1-T4), adiabatic section (T5-T6), condensing section (T7-T10) and inlet and outlet water temperature of cooling water in condensing section (T_{wa1} and T_{wa2}) were tested.

In order to study the phenomenon of dryout, we manufactured four different liquid filled heat pipes: 2ml, 3ml, 4ml and 5ml, corresponding to liquid FR of 1.08% , 1.62 % , 2.16 % and 2.7 % respectively. The R was calculated by the following formula:

$$R = \frac{T_e - T_c}{Q}$$

Heat transfer can be calculated from the inlet and outlet water temperature of cooling water in the condensing section:

$$Q = m_e c_p (T_{wa2} - T_{wa1})$$

Due to a series of insulation measure, the heat loss is negligible.

3.1. Uncertainty analysis

Uncertainty analysis is necessary because of measurement errors in parameters including different temperatures and cooling water flow rates. The error of temperature and cooling water flow is shown in Table4.

Table4. Uncertainty of measuring device

The measurement data	Device	The uncertainty
Wall temperature	Type K thermocouple	±0.75%
The environment temperature	The thermometer	±0.1℃
Cooling water velocity	Rotameter	±0.5%

For composite variables such as heat transfer power and total thermal resistance, their relative uncertainty is usually calculated as follows:

$$\frac{u(Q)}{Q} = \sqrt{\left[\frac{u(V)}{V}\right]^2 + \frac{u^2(T_{wa2}) + u^2(T_{wa1})}{(T_{wa2} - T_{wa1})^2}}$$

$$\frac{u(R)}{R}=\sqrt{\left[\frac{u(Q)}{Q}\right]^2+\frac{u^2(T_e)+u^2(T_c)}{(T_e-T_c)^2}}$$

The maximum relative uncertainty of heat transfer power and total thermal resistance are 3.1% and 5.2% respectively, which can meet the requirements of calculation.

4. Results and discussion

4.1. Transient analysis

Performing transient analysis on TPCT can provide a deeper understanding of their start-up characteristics and allow for an evaluation of the system's thermal conductivity performance.

With the increase of heating water temperature, TPCTs of low liquid FR will appear dryout phenomenon, that is, there is no liquid working medium at the bottom of the evaporation section. As shown in Figure5, when the hot water reaches 75℃ and the filling amount is 2ml, the water will evaporate quickly. However, due to the low FR, the heated water will evaporate without falling back to evaporate again. The circulation causes the dryout phenomenon in TPCT. When the filling amount reaches 4ml, some condensed water will fall to the bottom of the evaporation section.

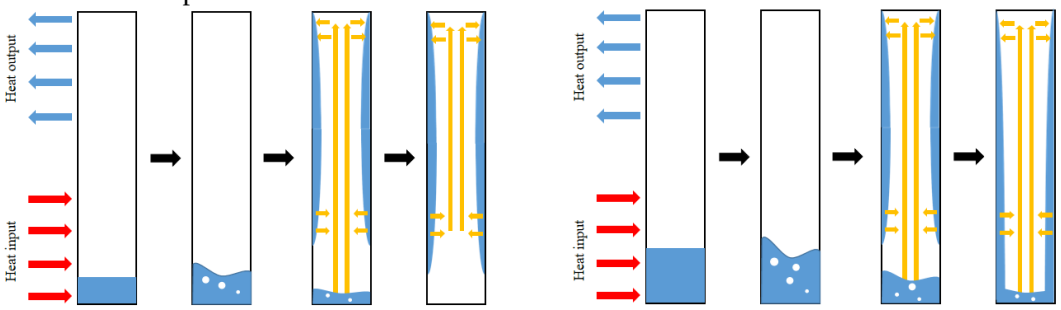

(a) 2ml (b) 4ml

Figure5. Schematic diagram of the variation of working medium in the TPCT when the heating temperature is 75℃ and the cooling water flow is 300L/h

4.2. The steady-state analysis

Conducting steady-state analysis on TPCTs can offer a comprehensive understanding of their heat transfer characteristics, enable evaluation of R, and ensure stable operating conditions.

4.2.1. Wall temperature distribution

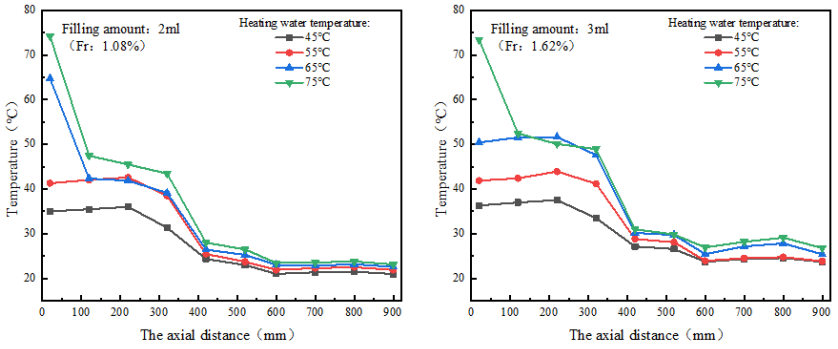

(a) Filling amount: 2ml (Fr=1.08%)

(b) Filling amount: 3ml (Fr=1.62%)

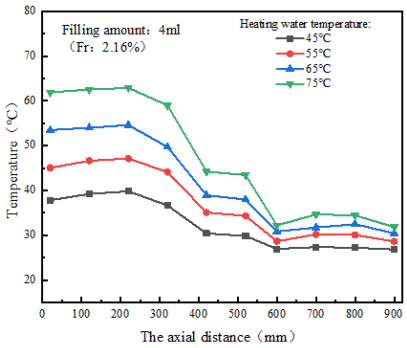

(c) Filling amount: 4ml (Fr=2.16%)

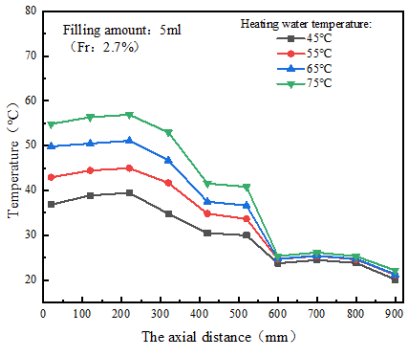

(d) Filling amount: 5ml (Fr=2.7%)

Figure6. Temperature distribution along the length of the thermosiphon at different liquid filling rates when the cooling water flow rate is 300L/h

As shown in Figure6, when the filling amount is 2ml and the temperature reaches 65℃, the phenomenon of dryout has occurred, the temperature at the measuring point T10 is close to the water temperature. However, when the filling amount is 3ml, only when the heating water temperature reaches 75℃ will appear the "evaporation" phenomenon; The TPCTs were able to operate properly in the experimental temperature range for liquid fillings up to 4ml and 5mL, but the 4ml TPCT had better isothermal properties. The temperature in the evaporation segments T2 and T3 is slightly higher than that of T1 and T4, which is due to the liquid reflux at T1 and T4 is located at the junction of the evaporative and adiabatic cross sections. As part of the condensed water passes through, the temperature is slightly reduced. The condensate evaporates before it reaches T2 and T3, so that T2 and T3 have slightly higher temperatures than T1 and T4. In the condensation cross section, the temperature of T8 and T9 is slightly higher than that of T7 and T10 due to the thin film of liquid in T8 and T9.

4.2.2. Heat transfer under different working conditions

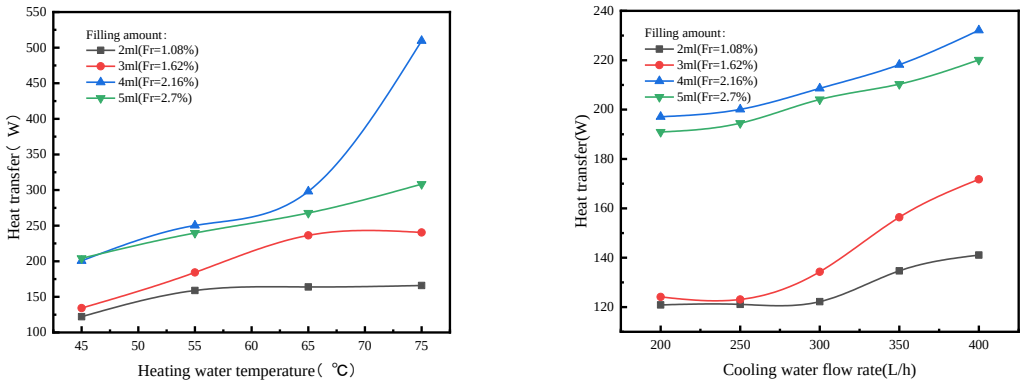

(a) (b)

Figure7. Heat transfer under different conditions

By changing the temperature of the heated water and the flow rate of the cooled water, the heat transfer difference between different liquid-filled TPCTs was compared. It can be seen from the Figure7(a) that by increasing the temperature of the heated water, the heat transfer is also increased. For the filling amount of 2ml, 3ml, and 4 ml, the increase of heat transfer did not change much with the increase of heating water temperature. When the filling amount reaches 5ml and the temperature of the heating water reaches 75℃, the heat transfer increases significantly. This is because at this point, the working medium evaporating from the evaporation cross section form a dynamical equilibrium with the working medium under the condensation cross section, and the heat transfer reaches its limit. The results showed that the heat transfer of the TPCTs with 2ml and 3ml liquid filling amount did not change significantly, that is, dryout occurred as described previously. When the filling amount is 5ml, there is still a small amount of liquid at the bottom of the TPCT.

It can be seen from the Figure7(b) that the increase of cooling water flow speeds up the heat transfer in the condensing section. The amount of fluid filling plays a decisive role in the variation of the heat transfer. When the filling amount was increased from 3ml to 4ml, the flow state in the TPCT changes drastically, resulting in a sharp increase in heat transfer. The TPCTs with the liquid amount of 2ml and 3ml change significantly with the change of cooling water, this is due to the low liquid amount of TPCT is more vulnerable to changes in the external conditions, the flow of the internal situation is more complicated.

4.2.3. Thermal resistance

The thermal resistance network model is established based on theoretical derivations and assumptions, enabling the calculation of the contributions of various R components in the heat conduction paths under different operating conditions using mathematical methods. This allows for the evaluation of the model's capability to describe real systems.

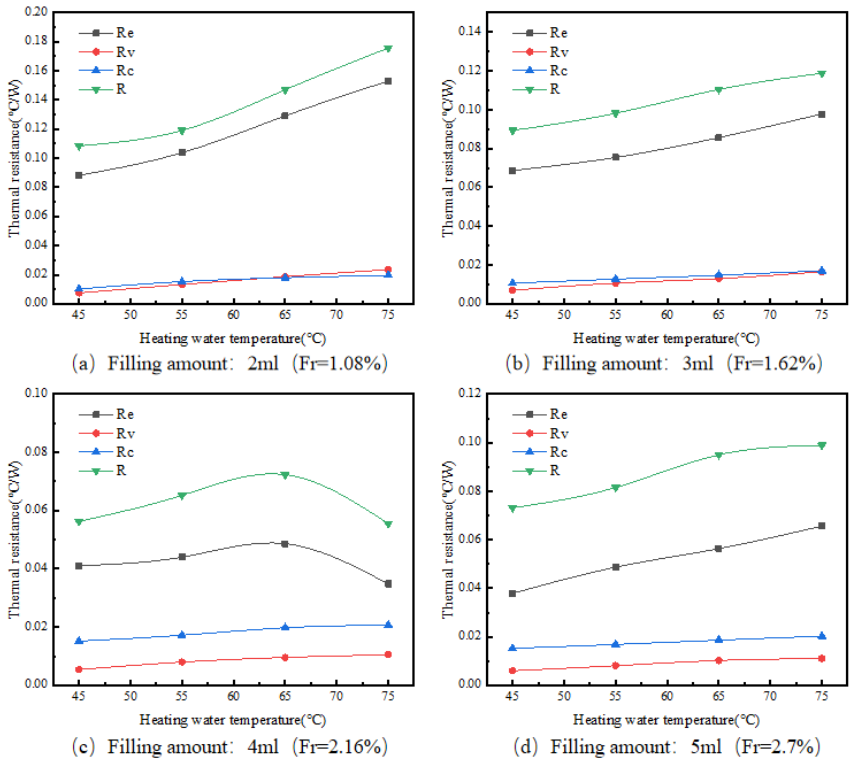

Figure8. The R of the TPCT under different heating water temperature in steady state when the cooling water flow rate is 300L/h

As shown in Figure8, for the filling amount of 2ml, the total thermal resistance of the TPCT increases with the heating water temperature. When the amount of liquid is 2ml and 3ml, the total R of the TPCT increases and then tends to be constant. The total R of the TPCT increases and then decreases when the liquid amount is 5ml.

In other words, when the temperature reaches 65℃, there is an "inflection point". This is because when the heating water temperature reaches 65℃, the phenomenon of dryout occurs in the TPCTs filled with 2ml and 3mL liquid. When the change in heat transfer is small, the temperature difference between the evaporation and condensation cross sections is large, and thus the R increases. Evaporation is more obvious when the liquid filling amount is 2mL, and thus the increasing trend is more pronounced.

However, when the liquid filling amount is 5ml, there will be no dryout phenomenon, but the increasing trend of temperature difference is always greater than that of heat transfer, so the R gradually increases. When the liquid amount is 4ml, no dryout phenomenon occurs, but when the temperature of the heated water reaches 75℃, the heat transfer increases sharply, resulting in a decrease in R.

At the same time, it is not hard to see that the variation trend of total R is consistent with that of evaporation R. The R of steam flow and condensing section increases slightly with the increase of heating water temperature, but has little effect on the total R.

5. Experimental and empirical comparison of thermal resistance

Comparing the R calculated by the network model with the experimentally calculated R can reveal the accuracy of experimental results and potential sources of errors. If the experimentally calculated R matches well with the R calculated by the network model, it indicates a

higher reliability of the experimental data and the ability of the R network model to effectively explain the thermal conduction behavior of the actual system.

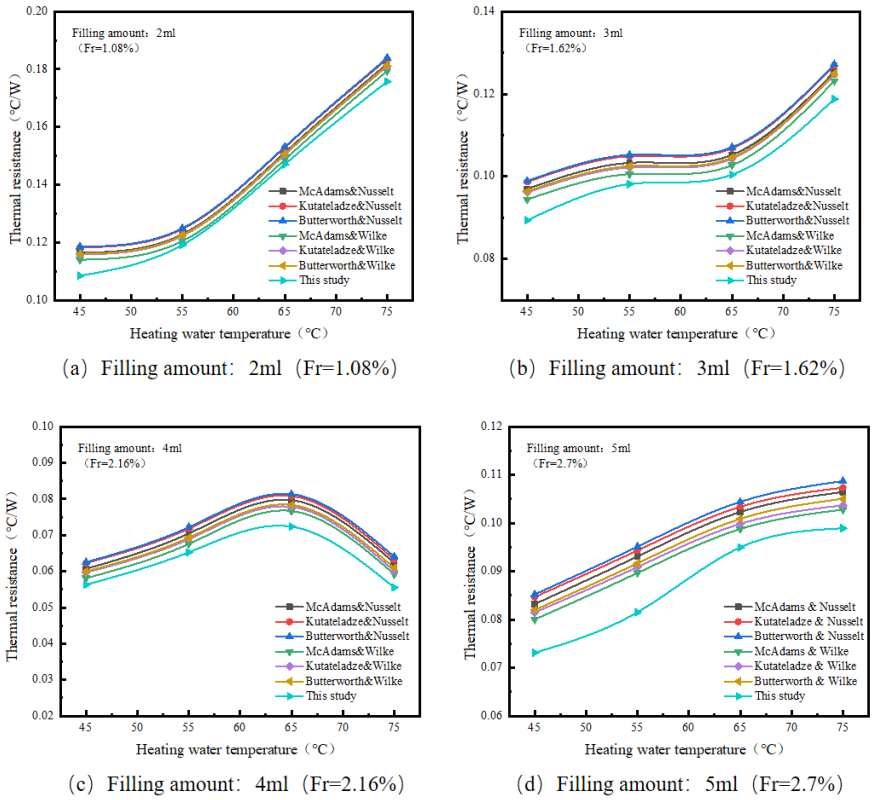

(a) Filling amount: 2ml (Fr=1.08%) (b) Filling amount: 3ml (Fr=1.62%)

(c) Filling amount: 4ml (Fr=2.16%) (d) Filling amount: 5ml (Fr=2.7%)

Figure 9. Comparisons of empirical formulas and experimental data at different heating water temperatures when the cooling water flow rate is 300L/h

The R calculated from the empirical formula is compared with the one calculated in practice. The thermal drag calculated by the empirical formula is smaller than the one predicted by the empirical formula. The behavior of the bubbles may have a significant impact on the heat transfer properties. As the FR increases, the error becomes larger. This is because the internal flow pattern of the TPCT changes more as the fluid FR increases, which cannot be predicted accurately by the empirical formula.

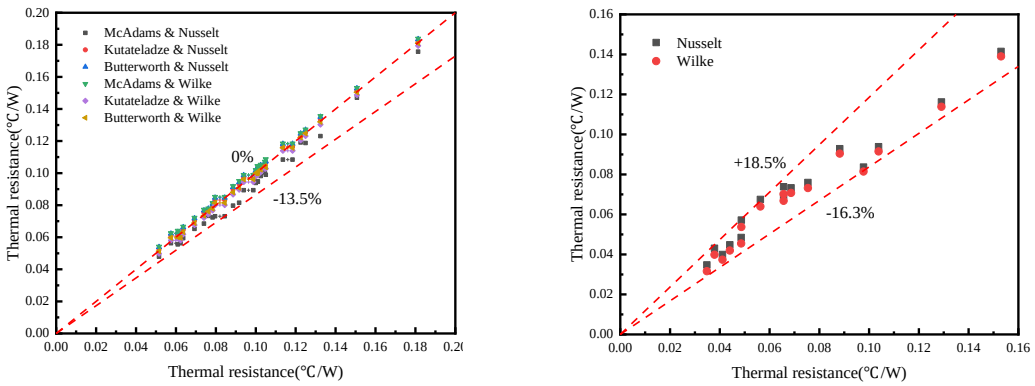

(a) (b)

Figure10. Errors between empirical formula and experimental result

As shown in Figure10(a), the deviation between the experimental results and the prediction of the R for different heating water temperatures and different cooling water flows is within 13.5 percent. This small deviation indicates that the R network model used is reliable and the experimental system performs well and is highly reliable.

As can be seen from Figure10(b), the deviation between the experimental results and the predictions for the thermal drag in the evaporation cross section is between -16.3% and 18.5% for different heating water temperatures and cooling water flow rates. This small deviation indicates that the formula for calculating the R of the evaporation cross section is also reliable, and that the chosen empirical formula can also be applied to the model.

The total R obtained by this formula is always smaller than the one obtained by the empirical formula. Although the deviation of the evaporation cross section from the total R is larger, it does not mean that the evaporation cross section is inaccurately calculated. Although the deviation of the thermal drag from the condensation cross section is larger than that of the evaporation cross section, it is still within the allowed errors. Therefore, we can argue that our model of the thermistor network may overpredict the thermistor of the steam flow, whereas the empirical formula for the thermistor of the steam flow is not that large in practice.

6. Conclusion

(1) When the liquid charged in the TPCT is too low, dryout may occur in the TPCT with high heat flow ratio, resulting in a sharp increase in R. Therefore, the TPCTs must be kept in a normal working state.

(2) As the heating water temperature and the cooling water flow rate increase, the heat transfer from the TPCT increases. A TPCT with 4ml of liquid filling has the best performance: better isotherm, greater heat transfer and minimum R under the same working conditions.

(3) The trend of the R is closely related to the amount of liquid filling and the temperature of the hot water, and the variation of the R with the flow of the cooling water is small. This is because a change in the amount of liquid filling and the temperature of the heated water can drastically change the flow state of the tube, especially for TPCTs with small amounts of liquid filling.

(4) The change of the total R is consistent with the R of the evaporation section. With the increase of hot water temperature, the R of steam flow and condensing section increases slightly, but has no effect on the change trend of total R.

(5) The R derived from the empirical formula is in good agreement with the experimental data. The actual results are always slightly smaller than those obtained by the empirical formula, which is due to the over-prediction of the R of the vapor flow.

Nomenclature

A	-area [m^2]	Greek symbols	
c_p	-specific heat capacity of fluid, [$J \cdot kg^{-1} \cdot K^{-1}$]	λ	-thermal conductivity, [$W \cdot m^{-1} \cdot K^{-1}$]
D	-equivalent diameter, [mm]	ρ	-fluid density, [$kg \cdot m^{-3}$]
Fr	-fill ratios	μ	-dynamic viscosity, [Pa·s]
g	-gravity, [$m \cdot s^{-2}$]	ω	-angular velocity, [rad/s]
h	-heat transfer coefficient, [$W \cdot m^{-2} \cdot K^{-1}$]	δ	-thickness
m_e	-mass flow rate, [$Kg \cdot h^{-1}$]	Subscripts	
p	-pressure, [Pa]	*ext*	-external
q	-heat flux, [$W \cdot m^{-2}$]	*in*	-inlet

Q	-heat transfer, [W]	*out*	-outlet
R	-thermal resistance[$K \cdot W^{-1}$]	*u, v, w*	-direction of coordinate
Ref	-Reynolds number	*e*	-evaporator
T	-temperature, [℃]	*a*	-adiabatic
TPCT	-two-phase closed thermosiphon	*c*	-condensation
wall	-tube wall	*vap*	-vapor

Acknowledgement

The computational resources generously provided by the High Performance Computing Center of Nanjing Tech University are greatly appreciated.

References

[1] Faghri A. Heat pipe science and technology. Global Digital Press, 1995.

[2] Reay D, McGlen R, Kew P. Heat pipes: theory, design and applications. Butterworth-Heinemann, 2013.

[3] Alizadeh M, Ganji D D. Heat transfer characteristics and optimization of the efficiency and thermal resistance of a finned thermosyphon. Applied Thermal Engineering, 2021, 183: 116136.

[4] Alammar A A, Al-Dadah R K, Mahmoud S M. Experimental investigation of the influence of the geyser boiling phenomenon on the thermal performance of a two-phase closed thermosyphon. Journal of cleaner production, 2018, 172: 2531-2543.

[5] Chen X, Jiang F, Qi G, et al. Experimental investigation on a three-phase closed thermosyphon with glass beads/water. Applied Thermal Engineering, 2019, 154: 157-170.

[6] Mozumder A K, Akon A F, Chowdhury M S H, et al. Performance of heat pipe for different working fluids and fill ratios. Journal of Mechanical Engineering, 2010, 41(2): 96-102.

[7] Guichet V, Delpech B, Khordehgah N, et al. Experimental and theoretical investigation of the influence of heat transfer rate on the thermal performance of a multi-channel flat heat pipe. Energy, 2022, 250: 123804.

[8] Zhang M, Yan Z, Pei W, et al. Experimental study on the startup and heat transfer behaviors of a two-phase closed thermosyphon at subzero temperatures. International Journal of Heat and Mass Transfer, 2022, 190: 122283.

[9] Mozumder A K, Akon A F, Chowdhury M S H, et al. Performance of heat pipe for different working fluids and fill ratios. Journal of Mechanical Engineering, 2010, 41(2): 96-102.

[10] Guichet V, Jouhara H. Condensation, evaporation and boiling of falling films in wickless heat pipes (two-phase closed thermosyphons): a critical review of correlations. International Journal of Thermofluids, 2020, 1: 100001.

[11] Nusselt W. Die oberfluchenkondensation des wasserdampfes. Z. VDI, 1916, 60(28): 569.

[12] Transmission H. by WH McAdams[J]. McGraw-Hill Book Co., New York, 1942, 214.

[13] Kutateladze S S. Heat transfer theory fundamentals. 1963.

[14] Butterworth C. Condensers: Basic heat transfer and fluid flow. Kakaç, S.; Bergles, AE; Mayinger, F.: Heat exchangers: Thermal-hydraulic fundamentals and design. Washington: Hemisphere, 1981: 289-313.

[15] Rohsenow W M, Hartnett J P, Cho Y I. Handbook of heat transfer. New York: McGraw-Hill, 1998.

[16] Cengel Y A, Klein S, Beckman W. Heat transfer: a practical approach. Boston: WBC McGraw-Hill, 1998.

[17] Nusselt W. Die oberfluchenkondensation des wasserdampfes. Z. VDI, 1916, 60(28): 569.
[18] Wilke W. Wärmeübergang an Rieselfilme: Mitteilung d. Forschungsgruppe f. Wärme-u.
[19] Chun K R, Seban R A. Heat transfer to evaporating liquid films. 1971.
[20] Fujita T, Ueda T. Heat transfer to falling liquid films and film breakdown—I: Subcooled liquid films. International Journal of Heat and Mass Transfer, 1978, 21(2): 97-108.

Paper submitted: 16 September 2023
Paper revised: 07 November 2023
Paper accepted: 08 November 2023